

A generalized confusion matrix for assessing area estimates from remotely sensed data

H. G. LEWIS

Astronautics Research Group, School of Engineering Sciences—Aeronautics and Astronautics, University of Southampton, Southampton SO17 1BJ, England, UK; e-mail: hglewis@soton.ac.uk

and M. BROWN

Unilever Research Port Sunlight, Quarry Road East, Bebington, Wirral L63 3JW, England, UK; e-mail: Martin.Q.Brown@unilever.com

(Received 14 August 1998; in final form 25 February 2000)

Abstract. The formulation of a generalized area-based confusion matrix for exploring the accuracy of area estimates is presented. The generalized confusion matrix is appropriate for both traditional classification algorithms and sub-pixel area estimation models. An error matrix, derived from the generalized confusion matrix, allows the accuracy of maps generated using area estimation models to be assessed quantitatively and compared to the accuracies obtained from traditional classification techniques. The application of this approach is demonstrated for an area estimation model applied to Landsat data of an urban area of the United Kingdom.

1. Introduction

The classification of remotely sensed data is an important use of satellite sensor technology for Earth observation. A significant number of applications rely on the accurate classification of such data. These include the mapping of land cover (Kanellopoulos *et al.* 1992), cloud categorization for weather forecasting (Pankiewicz 1997) and flood detection and monitoring (Profeti and MacIntosh 1997). In many cases high classification accuracies are required to establish and monitor economic, social or environmental policy. Where remotely sensed data have been considered for future monitoring of the landscape, for example, it has been suggested that an acceptable accuracy limit for land cover maps derived from the classification of satellite data is 85% (Anderson *et al.* 1976, Wright and Morrice 1997).

Accuracy assessment is typically achieved by comparing the classifications made by an algorithm to the known classifications at selected, sampled reference locations. The sampled data are then characterized in a confusion matrix and a variety of descriptive and analytical measures can be used to summarize the accuracy of classification (Card 1982, Congalton 1991, Richards 1996, Stehman 1997). If the composition of the sampled data represents true class proportions in the image scene then these measures are reliable estimates of the accuracy of the classified scene (Richards 1996). Using an iterative proportional fitting procedure, which forces each

row and column to sum to one, the differences in sample sizes used to generate matrices are removed and individual cell values within the matrix are comparable (Congalton 1991). In addition, normalized matrices can also be used to directly compare cell values between matrices produced using different classification algorithms (Stehman 1997).

The confusion matrix is appropriate for traditional methods of classification where it is assumed that pixels at the reference locations can be assigned to single classes, and accuracy measures based on the proportion of area correctly classified are then calculated from the number of pixels that are correctly classified. However, it has been suggested that this assumption is not appropriate for representing real situations because several classes may occur in the instantaneous field of view of the satellite sensor represented by a single pixel (Horwitz *et al.* 1971, Foody and Cox 1994).

Linear spectral mixture models were proposed to improve the accuracy of classification (Horwitz *et al.* 1971) and have since been applied to the analysis of remotely sensed data for mapping land cover proportions (Adams *et al.* 1986, Settle and Drake 1993, Garcia-Haro *et al.* 1996) and for cloud fraction retrievals (Arai *et al.* 1995). The approach taken by these models is to explicitly represent the mixing in pixels as fuzzy memberships in the unit range (Robinson and Thongs 1986, Foody and Cox 1994). Alternative, nonlinear approaches to unmixing pixels, which make no assumptions about the nature of the mixing, have used artificial neural networks (Atkinson *et al.* 1997, Foody *et al.* 1997). In both cases, pixels are assigned a fuzzy membership of all classes where the membership represents a sub-pixel proportion of area (Fisher and Pathirana 1990, Cross *et al.* 1991, Manslow *et al.* 2000).

Area estimates produced using mixing models have been shown to be more accurate than area estimates derived using traditional classification methods (Foody 1996). However, (Foody 1996, p. 1325) suggests that 'the measures of classification accuracy derived from the confusion matrix are inappropriate for the evaluation of fuzzy classifications' since the assumption that a pixel can be allocated correctly or incorrectly to a single class no longer holds. For example, two typical measures that are reported are the producer's accuracy and the user's accuracy (Story and Congalton 1986). The producer's accuracy is related to the error of commission and the user's accuracy is related to the error of omission (Congalton 1991). The unsuitability of these measures for area estimation models has led to the use of alternative assessment methods that are not based on the confusion matrix. For example, a measure of closeness (Foody 1996) and measures of entropy (Finn 1993, Maselli *et al.* 1994). Whilst these alternatives allow the comparison of traditional classification algorithms to sub-pixel area estimation models, they are not as familiar to the users of the classified map as the measures derived from the confusion matrix, or the confusion matrix itself. In addition, the use of these alternative measures alone obscures potentially important details about problematic classes that are contained in a confusion matrix (Stehman 1997). In response to these limitations, Gopal and Woodcock (1994) reported a method for the assessment of area estimates using confusion matrices and fuzzy sets. Their approach, however, used MAX and RIGHT (threshold) functions to first encode pixel area estimates as single classes in order to generate the confusion matrices.

This article proposes that confusion matrices represent a valid approach to accuracy assessment of area estimates, and that a generalized area-based confusion matrix can be used to describe errors in the estimation of classes' areas. The approach uses a reference matrix, which describes the pure and mixed classes in the target

reference data, to represent explicitly the errors in the modelled class mixing represented by the confusion matrix. Complimentary summary measures are described that are appropriate for the area-based interpretation of the data. Throughout the article, data produced from a hypothetical classification algorithm and a hypothetical area estimation model are used to illustrate the suitability of the approach. The assessment of an area estimation model applied to an urban area of Leicester in the United Kingdom is also presented as an example.

2. Categorical and area-based interpretation of image pixels

Traditional classification methods assume that pixels contain only a single class and that the classification algorithm can assign a class label exclusively to each pixel. The target reference data and the output data reflect this assumption and are usually encoded using a binary, one-out-of-*c* classes scheme (Bishop 1995). In the target data, therefore, a pixel is assigned a membership of one in the target class and zero in every other class to form a closed-world, mutually exclusive set. Statistical classification algorithms typically produce estimates of the membership that are less than one and these values can be interpreted as *a posteriori* probabilities. The class having the highest *a posteriori* probability is then assigned to the pixel. Other methods assign pixels to classes according to the location of the pixel feature vector, with respect to a separating hyperplane, in the feature space. The output data produced by all of these methods can be meaningfully described using the one-out-of-*c* binary encoding scheme.

Area estimation methods, such as the linear mixture model, assume that a pixel contains spectral information received at the satellite from a physical surface area containing a single class or a mixture of classes that fills the pixel. In this case, fuzzy memberships that are equivalent to the proportion of area containing each class are used to describe the mixing within the pixel (Fisher and Pathirana 1990, Cross *et al.* 1991, Manslow *et al.* 2000). An area estimation model performs the process of assigning class area proportions to pixels. An area-based encoding scheme assigns each pixel of the data a membership of all *c* classes, where the memberships (*i*) represent area proportions, (*ii*) are real positive values in the range [0, 1] and (*iii*) sum (over all classes) to unity. Target memberships for a pixel can be presented in a $1 \times c$ target vector, **t**, and, similarly, the memberships produced by the area estimation model can be presented in a $1 \times c$ output vector, **y**. Target information can be derived from manual interpretation of high-resolution digitized aerial photographs, or field surveys. The sum-to-unity constraint imposed upon the memberships of each pixel implies a closed world. That is, the classes contained in the dataset are appropriate for, and representative of, the classes found in the real-world scene. In some cases it may be necessary to include classes that are not useful to the user, such as shadow (Adams *et al.* 1986), in order to meet this closed-world assumption.

3. Derivation of a generalized area-based confusion matrix

For area estimation models, the memberships in a target reference dataset containing *m* pixels and *c* classes can be presented in an $m \times c$ target matrix, **T**, where

$$\mathbf{T} = \begin{bmatrix} \mathbf{t}_1 \\ \mathbf{t}_2 \\ \vdots \\ \mathbf{t}_m \end{bmatrix} = \begin{bmatrix} t_{11} & t_{12} & \cdots & t_{1c} \\ t_{21} & t_{22} & & t_{2c} \\ \cdots & & \ddots & \vdots \\ t_{m1} & t_{m2} & \cdots & t_{mc} \end{bmatrix} \tag{1}$$

and $\sum_{j=1}^c t_{kj} = 1$ for $k=1, \dots, m$. Similarly, the memberships assigned to the m pixels by the model can be presented in an $m \times c$ output matrix, \mathbf{Y} , where

$$\mathbf{Y} = \begin{bmatrix} \mathbf{y}_1 \\ \mathbf{y}_2 \\ \vdots \\ \mathbf{y}_m \end{bmatrix} = \begin{bmatrix} y_{11} & y_{12} & \cdots & y_{1c} \\ y_{21} & y_{22} & & y_{2c} \\ \cdots & & \ddots & \vdots \\ y_{m1} & y_{m2} & \cdots & y_{mc} \end{bmatrix} \tag{2}$$

and $\sum_{j=1}^c y_{kj} = 1$ for $k=1, \dots, m$. The $c \times c$ area-based confusion matrix, \mathbf{C} , can then be derived from the outer product of the transpose of the target matrix, \mathbf{T} and the output matrix, \mathbf{Y} ,

$$\mathbf{C} = \mathbf{T}^T \mathbf{Y} = \begin{bmatrix} \sum_{k=1}^m t_{k1} y_{k1} & \sum_{k=1}^m t_{k1} y_{k2} & \cdots & \sum_{k=1}^m t_{k1} y_{kc} \\ \sum_{k=1}^m t_{k2} y_{k1} & \sum_{k=1}^m t_{k2} y_{k2} & & \sum_{k=1}^m t_{k2} y_{kc} \\ \vdots & & \ddots & \vdots \\ \sum_{k=1}^m t_{kc} y_{k1} & \sum_{k=1}^m t_{kc} y_{k2} & \cdots & \sum_{k=1}^m t_{kc} y_{kc} \end{bmatrix} \Rightarrow \begin{bmatrix} \sum_{k=1}^m t_{k1} \\ \sum_{k=1}^m t_{k2} \\ \vdots \\ \sum_{k=1}^m t_{kc} \end{bmatrix} \tag{3}$$

$$\Downarrow$$

$$\begin{bmatrix} \sum_{k=1}^m y_{k1} & \sum_{k=1}^m y_{k2} & \cdots & \sum_{k=1}^m y_{kc} \end{bmatrix}$$

where the row and column sums are represented in the vectors that are also shown.

Whilst the individual elements of this area-based confusion matrix cannot be interpreted as areas, the row and column sums shown in (3) can be interpreted in this manner. The sum of the elements in row i of the confusion matrix, \mathbf{C} , is

$$\sum_{j=1}^c C_{ij} = \sum_{k=1}^m \sum_{j=1}^c t_{ki} y_{kj} = \sum_{k=1}^m \left(t_{ki} \sum_{j=1}^c y_{kj} \right) = \sum_{k=1}^m t_{ki} \tag{4}$$

This is the total area covered by class i in the target reference data, for the closed-world assumption on the output data (i.e. $\sum_{j=1}^c y_{kj} = 1$). Similarly, it can be shown that the sum of the elements in column j corresponds to the total area covered by class j in the output data for the closed-world assumption on the target data.

The area-based confusion matrix derived using (3) is a different interpretation of the confusion matrix that is traditionally produced and reported for binary encoded classified samples. The example, described below, uses data from a hypothetical classification scheme (table 1) to illustrate this property. An additional example presents the area-based confusion matrix for data produced by a hypothetical area estimation model (table 2).

3.1. Area-based confusion matrix from binary encoded data

The confusion matrix, \mathbf{C} , for the binary encoded data in table 1 produced by a hypothetical classification scheme was derived from (3) to give,

Table 1. Binary encoded data for three classes, *a*, *b* and *c*.

Pixel	Target matrix T			Output matrix Y		
	<i>a</i>	<i>b</i>	<i>c</i>	<i>a</i>	<i>b</i>	<i>c</i>
1	1	0	0	1	0	0
2	1	0	0	1	0	0
3	1	0	0	0	1	0
4	0	1	0	0	1	0
5	0	1	0	0	1	0
6	0	1	0	0	0	1
7	0	0	1	0	0	1
8	0	0	1	0	0	1
9	0	0	1	1	0	0
10	0	0	1	0	1	0

Table 2. Area-based encoded data for three classes, *a*, *b* and *c*.

Pixel	Target matrix T			Output matrix Y		
	<i>a</i>	<i>b</i>	<i>c</i>	<i>a</i>	<i>b</i>	<i>c</i>
1	0.8	0.1	0.1	0.7	0.2	0.1
2	0.6	0.3	0.1	0.6	0.4	0.0
3	0.9	0.0	0.1	0.8	0.1	0.1
4	0.2	0.6	0.2	0.3	0.6	0.1
5	0.1	0.7	0.2	0.1	0.7	0.2
6	0.0	0.6	0.4	0.1	0.4	0.5
7	0.0	0.0	1.0	0.0	0.1	0.9
8	0.1	0.3	0.6	0.2	0.2	0.6
9	0.0	0.2	0.8	0.1	0.1	0.8
10	0.3	0.2	0.5	0.4	0.2	0.4

$$\mathbf{C} = \begin{bmatrix} 2 & 1 & 0 \\ 0 & 2 & 1 \\ 1 & 1 & 2 \\ 3 & 4 & 3 \end{bmatrix} \begin{bmatrix} 3 \\ 3 \\ 4 \end{bmatrix} \tag{5}$$

The interpretation of the elements of the area-based confusion matrix is simple, and equivalent to the interpretation of the traditional confusion matrix, for binary encoded data (Congalton 1991). The row sums in (3) indicate the number of whole pixels assigned to each of the three classes in the target dataset and the column sums in (3) represent the number of pixels assigned to the classes by the classification algorithm. The diagonal elements represent the number of pixels correctly classified for each class and the off-diagonal elements represent errors of omission or commission. Assessment of the area estimates for each class can be made from the whole number of pixels in each element, or in the row and column sums, of the matrix.

3.2. Area-based confusion matrix from sub-pixel area estimates

The confusion matrix, **C**, for the data produced by a hypothetical area estimation model (in table 2), was derived from (3) to give

$$\mathbf{C} = \begin{bmatrix} 1.85 & 0.76 & 0.39 \\ 0.72 & 1.35 & 0.93 \\ 0.73 & 0.89 & 2.38 \\ [3.3 & 3.0 & 3.7] \end{bmatrix} \begin{bmatrix} 3 \\ 3 \\ 4 \end{bmatrix} \tag{6}$$

Here, the individual elements of the confusion matrix can no longer be interpreted straightforwardly because there is no longer a concept of correct or incorrect classification. However, the row sums and column sums define the target areas and the estimated areas of the classes, respectively, and these values can be used to assess the accuracy of the area estimates.

The elements of the area-based confusion matrix describe the strength of correspondence between the target class areas and the estimated class areas and, also, they implicitly describe the strength of pure classes and mixtures of classes in the data. For ideal area estimation models the target and estimated class areas are the same and the confusion matrix is symmetrical and simply describes the strength of mixing of classes in the data. This ideal confusion matrix is equivalent to the $c \times c$ reference matrix, \mathbf{R} , calculated from the target reference data,

$$\mathbf{R} = \mathbf{T}^T \mathbf{T} \tag{7}$$

since, in this case, $y_{ki} = t_{ki} \forall k, i$. The reference matrix reflects the distribution of class mixtures that occurs in the target data and this matrix can be used to determine if the target data are complete (i.e. the distribution of class mixtures in the target data is equivalent to the distribution in the real scene). The row and column sums of \mathbf{R} are equal and correspond to the total area covered by each class in the target reference data.

Generally, area estimation models are not ideal and errors are apparent in a confusion matrix that is not symmetrical and that differs from the ideal, symmetrical reference matrix. The differences between the reference matrix, \mathbf{R} , and the confusion matrix, \mathbf{C} , for target and output data can be represented explicitly in an error matrix.

4. The error matrix

The error matrix, \mathbf{E} , which quantifies the differences of the confusion matrix, \mathbf{C} , from the reference matrix, \mathbf{R} , is

$$\mathbf{E} = \mathbf{R} - \mathbf{C}$$

$$= \begin{bmatrix} \sum_{k=1}^m t_{k1}(t_{k1} - y_{k1}) & \sum_{k=1}^m t_{k1}(t_{k2} - y_{k2}) & \cdots & \sum_{k=1}^m t_{k1}(t_{kc} - y_{kc}) \\ \sum_{k=1}^m t_{k2}(t_{k1} - y_{k1}) & \sum_{k=1}^m t_{k2}(t_{k2} - y_{k2}) & & \sum_{k=1}^m t_{k2}(t_{kc} - y_{kc}) \\ \vdots & & \ddots & \vdots \\ \sum_{k=1}^m t_{kc}(t_{k1} - y_{k1}) & \sum_{k=1}^m t_{kc}(t_{k2} - y_{k2}) & \cdots & \sum_{k=1}^m t_{kc}(t_{kc} - y_{kc}) \end{bmatrix} \Rightarrow \begin{bmatrix} \sum_{j=1}^c E_{1j} = 0 \\ \sum_{j=1}^c E_{2j} = 0 \\ \vdots \\ \sum_{j=1}^c E_{cj} = 0 \end{bmatrix}$$

$$\Downarrow$$

$$\left[\begin{array}{cccc} \sum_{k=1}^m (t_{k1} - y_{k1})t_{k1} & \sum_{k=1}^m (t_{k2} - y_{k2})t_{k1} & \cdots & \sum_{k=1}^m (t_{kc} - y_{kc})t_{k1} \end{array} \right] \tag{8}$$

where the row and column sums are represented in the vectors that are also shown.

Whilst each element of the error matrix derived using (8) cannot be interpreted as an absolute error in the estimated area, this matrix does quantify the relative errors in the estimation of pure and mixed classes' areas. Pixels containing a pure class or a mixture of classes, whose areas the model correctly estimates (i.e. pixels for which $t_{kj} = y_{kj}$) will contribute a value of zero to the error matrix. Pixels that are incorrectly modeled ($t_{kj} \neq y_{kj}$) will contribute either a negative or positive value to the error matrix. Therefore, values near to zero in the error matrix represent good area estimation and high (positive or negative) values represent poor area estimation by the model. Ideally, the value of all of the elements of the error matrix would be zero. This would correspond to the case where the area estimates are equal to the target areas for every pixel and every class.

Assuming a closed world on the target and output data (i.e. $\sum_{j=1}^c y_{kj} = 1$ and $\sum_{j=1}^c t_{kj} = 1$), the sum of elements in row i of the error matrix is zero and the sum of elements in column j of the error matrix is

$$\sum_{i=1}^c E_{ij} = \sum_{i=1}^c \left(\sum_{k=1}^m t_{ki}(t_{kj} - y_{kj}) \right) = \sum_{k=1}^m (t_{kj} - y_{kj}) \tag{9}$$

It is possible for the error in the area for a particular class calculated from the column sum (9) to be zero, but individual elements in the column may be non-zero. This signifies that the area estimates differ from the target areas for individual pixels, but when calculated over all the pixels the area estimate for the class is correct. Consequently, when reporting summary measures calculated from the column sum of the error matrix it is also necessary to report the full error matrix so that the summary measures may be seen in context. The absolute sum over the elements in column j of the error matrix

$$\sum_{i=1}^c |E_{ij}| = \sum_{i=1}^c \left| \sum_{k=1}^m t_{ki}(t_{kj} - y_{kj}) \right| \tag{10}$$

can also be used to highlight errors in the estimation of particular pure classes and mixtures of classes, even when the column sum (9) is zero.

The definition of the reference and error matrices for binary encoded data is trivial and is rarely done since no new information is gained. In this case the row sum of **C** is equivalent to the diagonal elements of **R**. Reference and error matrices for area-based encoded data carry meaningful information about problematic classes and mixtures of classes that cannot be found from the area-based confusion matrix alone. For illustration, the error matrix for the binary encoded data (in table 1) and the error matrix for the data produced by a hypothetical area estimation model (in table 2) are presented below.

4.1. Error matrix from binary encoded data

The reference matrix for binary encoded data has zero-valued non-diagonal elements and the diagonal elements correspond to the distribution of the classes in the target reference data. From (8), the error matrix for the binary encoded data in table 1 is

$$\mathbf{E} = \mathbf{R} - \mathbf{C} = \begin{bmatrix} 3 & 0 & 0 \\ 0 & 3 & 0 \\ 0 & 0 & 4 \end{bmatrix} - \begin{bmatrix} 2 & 1 & 0 \\ 0 & 2 & 1 \\ 1 & 1 & 2 \end{bmatrix} = \begin{bmatrix} 1 & -1 & 0 \\ 0 & 1 & -1 \\ -1 & -1 & 2 \end{bmatrix} \begin{bmatrix} 0 \\ 0 \\ 0 \end{bmatrix} \tag{11}$$

[0 -1 1]

No new information has been obtained from the calculation of the error matrix that is not already present in the confusion matrix, **C**. However, measures summarizing this error matrix can be used for comparison with measures derived from data representing area estimates, as described below.

4.2. Error matrix from sub-pixel area estimates

The error matrix derived for the data in table 2 is

$$\begin{aligned}
 \mathbf{E} = \mathbf{R} - \mathbf{C} &= \begin{bmatrix} 1.96 & 0.54 & 0.50 \\ 0.54 & 1.48 & 0.98 \\ 0.5 & 0.98 & 2.52 \end{bmatrix} - \begin{bmatrix} 1.85 & 0.76 & 0.39 \\ 0.72 & 1.35 & 0.93 \\ 0.73 & 0.89 & 2.38 \end{bmatrix} \\
 &= \begin{bmatrix} 0.11 & -0.22 & 0.11 \\ -0.18 & 0.13 & 0.05 \\ -0.23 & 0.09 & 0.14 \end{bmatrix} \begin{bmatrix} 0 \\ 0 \\ 0 \end{bmatrix} \\
 & \quad [-0.3 \quad 0.0 \quad 0.3]
 \end{aligned} \tag{12}$$

The column sums of the error matrix indicate that the area of class *a* was over-estimated by the model by an area of 0.3 pixels, the area of class *b* was correctly estimated, and the area of class *c* was underestimated by 0.3 pixels. The error matrix itself details where the errors occurred.

5. Summary measures

Summary measures traditionally provide either a single performance index for the entire confusion matrix or several measures can be used to summarize the classification accuracies for each class (Congalton 1991, Stehman 1997). However, as suggested by Foody (1996), these measures are not necessarily appropriate for models that predict sub-pixel class areas. In this latter context, a user is typically interested in knowing that a particular class covers a certain area within a scene (Dymond 1992) and an indication of the error associated with the estimation of that area is appropriate and usually sufficient. Additional information about the distribution of errors can also be obtained directly from the data using methods such as those suggested by Foody (1996). Measures of accuracy describing the proportion of area in error can be derived from the error matrix as described below.

The overall proportion of area in error calculated over all classes is

$$P = \frac{\sum_{j=1}^c \left| \sum_{i=1}^c E_{ij} \right|}{m} \tag{13}$$

where *m* is the total number of pixels in the dataset. This corresponds to the absolute sum of all the column totals in the error matrix, **E**, divided by the number of pixels in the data. The proportion of area in error calculated for class *j*:

$$P_j = \frac{\sum_{i=1}^c E_{ij}}{\sum_{k=1}^c t_{kj}} \tag{14}$$

corresponds to the total of column j in the error matrix, \mathbf{E} , divided by the total of column j in the reference matrix, \mathbf{R} . The sign of P_j indicates whether the class area was underestimated (positive) or overestimated (negative). These summary measures can be utilized to provide an effective basis on which the accuracy of several maps, or the performance of several models, can be compared directly. To illustrate this ability, the summary measures in (13) and (14) were calculated for the data in table 2 produced by the hypothetical area estimation model.

5.1. Summary measures for hypothetical area estimation

The absolute sum of the error matrix column totals for the hypothetical area estimates is

$$\sum_{j=1}^c \left| \sum_{i=1}^c E_{ij} \right| = 0.6 \tag{15}$$

and therefore the overall proportion of area in error, for all classes, is $P = 0.6/10 = 0.06$ for $m = 10$. The proportions of area in error for each class are $P_a = -0.1$, $P_b = 0$ and $P_c = 0.075$.

6. Assessment of area estimates of urban land cover in Landsat data

Area estimates of land cover classes occurring in 30 m (optimal) resolution Landsat Thematic Mapper (TM) data of south-east Leicester were produced using a K -nearest-neighbour (KNN) area estimation model (Lewis *et al.* 1998). Four land cover classes—developed (D), undeveloped (U), vegetation (V) and other (O)—were identified in three, digitized, 25 cm resolution aerial photographs of the same location. The developed class consisted of building and road materials, the undeveloped class consisted primarily of sand, water and bare soil, and the other class consisted of cover types that could not be identified from the aerial photography. These land cover classes were delineated and vectorized in the aerial photographs by a human expert and the resulting vector maps were rectified to the Landsat image coordinates. The proportions of Landsat pixels containing each land cover class were then quantified (Hughes *et al.* 1999). The Landsat data from channel 1 are shown as images in figure 1 and the land cover class proportions from part of this dataset are shown in figure 2.

Two-thirds of the data (1804 pixels) were randomly selected for exemplars. Each exemplar, corresponding to a single Landsat pixel, consisted of an input vector of digital counts (one count for each of the six channels of the Landsat imagery used) and a target vector of class proportions. The KNN area estimation model assigns class proportions to new pixels by, firstly, identifying the K exemplar input vectors having the lowest Euclidean distance from the new pixel's input vector and, secondly, calculating a linear, weighted average of the K exemplar class proportions (Lewis *et al.* 1998).

The remaining one-third of the data not used for exemplars (980 pixels) formed the test set. The reference matrix, \mathbf{R} , calculated from (7) for the test set target memberships was

$$\mathbf{R} = \begin{bmatrix} \text{[D} & \text{U} & \text{V} & \text{O]} \\ \left[\begin{array}{cccc} 229.295 & 2.214 & 84.714 & 41.885 \\ 2.214 & 9.93 & 9.319 & 0.267 \\ 84.714 & 9.319 & 388.018 & 25.572 \\ 41.885 & 0.267 & 25.572 & 24.814 \end{array} \right] \left[\begin{array}{c} 358.108 \\ 21.73 \\ 507.623 \\ 92.538 \end{array} \right] \\ \text{[358.108} & \text{21.73} & \text{507.623} & \text{92.538]} \end{bmatrix} \tag{16}$$

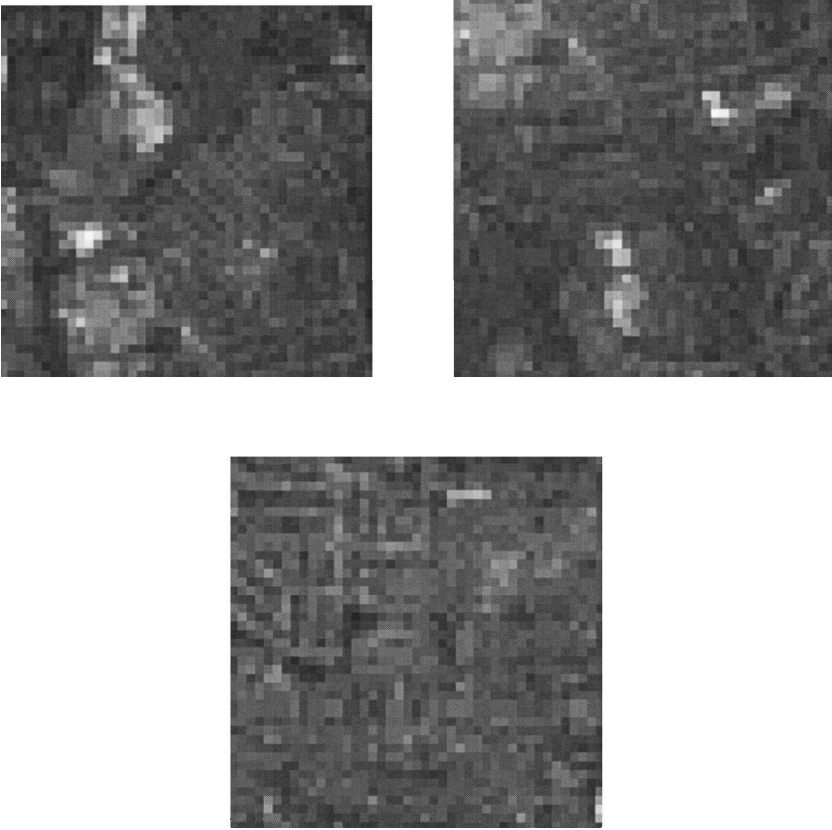


Figure 1. Landsat images of urban Leicester (channel 1).

This reference matrix indicated that the developed and vegetation classes were the most predominant (358.108 and 507.623 pixels respectively). The matrix also shows that the developed class mixed strongly with the vegetation class (column 1) and the other class mixed strongly with the developed class (column 4).

The generalized confusion matrix, **C**, calculated from (3) using the area estimates produced by the KNN area estimation model for the test set was

$$\mathbf{C} = \begin{bmatrix} \text{[D} & \text{U} & \text{V} & \text{O}]} \\ \begin{bmatrix} 198.995 & 2.5637 & 108.138 & 48.339 \\ 5.997 & 0.886 & 13.697 & 1.15 \\ 108.342 & 10.842 & 350.366 & 38.073 \\ 43.952 & 0.65 & 34.262 & 13.674 \end{bmatrix} \begin{bmatrix} 358.108 \\ 21.73 \\ 507.623 \\ 92.538 \end{bmatrix} \\ \text{[357.285} & \text{15.016} & \text{506.463} & \text{101.236]} \end{bmatrix} \tag{17}$$

The lack of symmetry of **C** indicates that there were some errors in the area estimates produced by the KNN model. These errors were quantified in the error matrix, **E**,

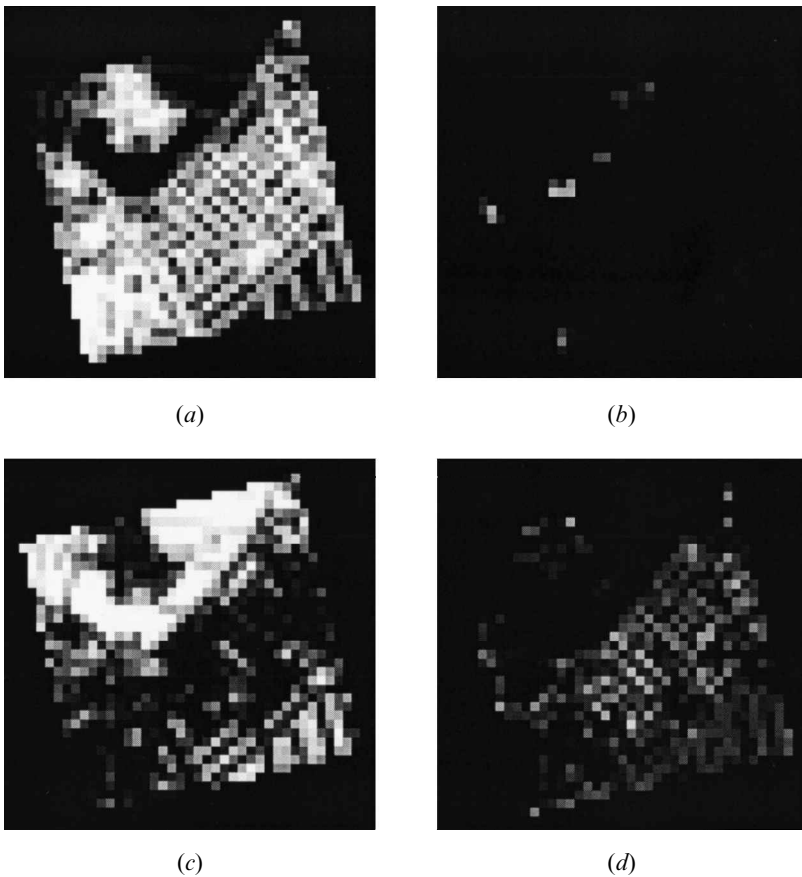


Figure 2. Class proportion images for the land cover classes (a) developed, (b) undeveloped, (c) vegetation and (d) other, in a Landsat image of Leicester. The grey level used for each pixel in these images is proportional to the area covered by the corresponding land cover class within each pixel.

calculated from the difference between (17) and (16):

$$\mathbf{E} = \begin{bmatrix} \text{D} & \text{U} & \text{V} & \text{O} \\ \begin{bmatrix} 30.3 & -0.423 & -23.424 & -6.454 \\ -3.783 & 9.044 & -4.378 & -0.883 \\ -23.628 & -1.523 & 37.652 & -12.501 \\ -2.067 & -0.383 & -8.69 & 11.14 \end{bmatrix} \\ \begin{bmatrix} 0 \\ 0 \\ 0 \\ 0 \end{bmatrix} \end{bmatrix} \quad (18)$$

$$\begin{bmatrix} 0.822 & 6.715 & 1.16 & -8.698 \end{bmatrix}$$

The error matrix is useful here because it indicates that the KNN area estimation model underestimates the areas associated with the pure classes (positive values on the diagonal) and overestimates the areas associated with mixtures of the classes (negative values off the diagonal).

The overall proportion of area in error, calculated from (13), is

$$P = (0.822 + 6.715 + 1.16 + 8.698)/980 = 0.0178 \quad (19)$$

and the proportions of area in error for each class, calculated from (14), are

$$P_{\text{developed}} = 0.822/358.108 = 0.0023 \quad (20a)$$

$$P_{\text{undeveloped}} = 6.715/21.73 = 0.309 \quad (20b)$$

$$P_{\text{vegetation}} = 1.16/507.623 = 0.0023 \quad (20c)$$

$$P_{\text{other}} = -8.698/92.538 = -0.094 \quad (20d)$$

A full analysis of these results and investigations into the sources of error in this example are beyond the scope of this article. This example, however, has demonstrated the use of the accuracy assessment technique based on the generalized confusion matrix described above for a real application.

7. Conclusions

The confusion matrix is a simple and popular method for describing classifier performance, yet it has not been adopted in the literature for the presentation of fuzzy classification results (Foody 1996). By assuming that sub-pixel classification can be interpreted as area estimation, this article has shown that a generalized area-based confusion matrix and a corresponding error matrix can be derived. Measures that summarize the information contained in this error matrix can then be used to compare the results of different classification methods and area estimation models.

Acknowledgments

This work is funded by the EC under the Framework 4, Environment and Climate Programme, as part of project FLIERS (Fuzzy Land Information from Environmental Remote Sensing, Contract number ENV4-CT96-0305). We thank Adrian Tatnall, John Manslow and Sarah Stevenage for helpful discussions.

References

- ADAMS, J., SMITH, M., and JOHNSON, P., 1986, Spectral mixture modeling: a new analysis of rock and soil types at the Viking Lander 1 site. *Journal of Geophysical Research*, **91**, 8098–8112.
- ANDERSON, J. R., HARDY, E. E., ROACH, J. T., and WITMER, R. E., 1976, A land use and land cover classification system for use with remote sensor data. US Geological Survey Professional Paper 964.
- ARAI, K., TERAYAMA, Y., UEDA, Y., and MORIYAMA, M., 1995, Adaptive least squares method for estimation of partial cloud coverage within a pixel. *International Journal of Remote Sensing*, **16**, 2197–2206.
- ATKINSON, P. M., CUTLER, M. E. J., and LEWIS, H., 1997, Mapping sub-pixel proportional land cover with AVHRR imagery. *International Journal of Remote Sensing*, **18**, 917–935.
- BISHOP, C. M., 1995, *Neural Networks for Pattern Recognition* (Oxford: Clarendon).
- CARD, D. H., 1982, Using known map category marginal frequencies to improve estimates of thematic map accuracy. *Photogrammetric Engineering and Remote Sensing*, **48**, 431–439.
- CONGALTON, R. G., 1991, A review of assessing the accuracy of classifications of remotely sensed data. *Remote Sensing of Environment*, **37**, 35–46.
- CROSS, A. M., SETTLE, J. J., DRAKE, N. A., and PAIVINEN, R. T. M., 1991, Subpixel measurement of tropical forest cover using AVHRR data. *International Journal of Remote Sensing*, **12**, 1119–1129.

- DYMOND, J. R., 1992, How accurately do image classifiers estimate area? *International Journal of Remote Sensing*, **13**, 1735–1742.
- FINN, J. T., 1993, Use of the average mutual information index in evaluating classification error and consistency. *International Journal of Geographical Information Systems*, **7**, 349–366.
- FISHER, P., and PATHIRANA, S., 1990, An evaluation of fuzzy memberships of landcover classes in the suburban zone. *Remote Sensing of the Environment*, **34**, 121–132.
- FOODY, G. M., 1996, Approaches for the production and evaluation of fuzzy land cover classifications from remotely-sensed data. *International Journal of Remote Sensing*, **17**, 1317–1340.
- FOODY, G. M., and COX, D. P., 1994, Sub-pixel land cover composition estimation using a linear mixture model and fuzzy membership functions. *International Journal of Remote Sensing*, **15**, 619–631.
- FOODY, G. M., LUCAS, R. M., CURRAN, P. J., and HONZAK, M., 1997, Non-linear mixture modelling without end-members using an artificial neural network. *International Journal of Remote Sensing*, **18**, 937–953.
- GARCIA-HARO, F. J., GILBERT, M. A., and MELIA, J., 1996, Linear spectral mixture modeling to estimate vegetation amount from optical spectral data. *International Journal of Remote Sensing*, **17**, 3373–3400.
- GOPAL, S., and WOODCOCK, C., 1994, Theory and methods for accuracy assessment of thematic maps using fuzzy sets. *Photogrammetric Engineering and Remote Sensing*, **60**, 181–188.
- HORWITZ, H. M., NALEPKA, R. F., HYDE, P. D., and MORGANSTERN, J. P., 1971, Estimating the proportion of objects within a single resolution element of a Multispectral Scanner. University of Michigan, Ann Arbor, Michigan, NASA Contract NAS-9-9784.
- HUGHES, M., BYGRAVE, J., BASTIN, L., and FISHER, P., 1999, High order uncertainty in spatial information: estimating the proportion of cover types within a pixel. In *Spatial Accuracy Assessment: Land information uncertainty in natural resources*, edited by K. Lowell and A. Jaton (Ann Arbor Press), pp. 319–323.
- KANELLOPOULOS, I., VARFIS, A., WILKINSON, G. G., and MÉGIER, J., 1992, Land-cover discrimination in SPOT HRV imagery using an artificial neural network—a 20-class experiment. *International Journal of Remote Sensing*, **13**, 917–924.
- LEWIS, H. G., BROWN, M., TATNALL, A. R. L., NIXON, M. S., and MANSLOW, J., 1998, Data analysis and empirical classification in FLIERS. Technical Report ISIS-3-98, Department of Electronics and Computer Science, University of Southampton, UK.
- MANSLOW, J. F., BROWN, M., and NIXON, M. S., 2000, On the probabilistic interpretation of area based fuzzy land cover mixing proportions. In *Artificial Neuronal Networks: Application to Ecology and Evolution*, edited by S. Lek and J.-F. Guégan (Berlin: Springer-Verlag), pp. 81–96.
- MASELLI, F., CONESE, C., and PETKOV, L., 1994, Use of probability entropy for the estimation and geographical representation of the accuracy of maximum likelihood classifications. *ISPRS Journal of Photogrammetry and Remote Sensing*, **49**, 13–20.
- PANKIEWICZ, G. S., 1997, Neural network classification of convective airmasses for a flood forecasting system. *International Journal of Remote Sensing*, **18**, 887–898.
- PROFETI, G., and MACINTOSH, H., 1997, Flood management through Landsat TM and ERS SAR data: a case study. *Hydrological Processes*, **11**, 1397–1408.
- RICHARDS, J. A., 1996, Classifier performance and map accuracy. *Remote Sensing of Environment*, **57**, 161–166.
- ROBINSON, V. B., and THONGS, D., 1986, Fuzzy set theory applied to the mixed pixel problem of multispectral landcover databases. In *Geographic Information Systems in Government*, edited by B. Opitz (Hampton, VA: A. Deepak), pp. 871–885.
- SETTLE, J. J., and DRAKE, N. A., 1993, Linear mixing and the estimation of ground cover proportions. *International Journal of Remote Sensing*, **14**, 1159–1177.
- STEHMAN, S. V., 1997, Selecting and interpreting measures of thematic classification accuracy. *Remote Sensing of Environment*, **62**, 77–89.
- STORY, M., and CONGALTON, R. G., 1986, Accuracy assessment: a user's perspective. *Photogrammetric Engineering and Remote Sensing*, **52**, 397–399.
- WRIGHT, G. G., and MORRICE, J. G., 1997, Landsat TM spectral information to enhance the land cover of Scotland 1988 dataset. *International Journal of Remote Sensing*, **18**, 3811–3834.